SUPPLEMENTARY INFORMATION

Near-infrared-photoinduced metamagnet based on a layered cyanido-bridged Co–W assembly with π–π interactions

Kazuki Nakamura,[a,b] Koji Nakabayashi,[a,b]* Shota Kobayashi,[a] and Shin-ichi Ohkoshi,[a,b]*

[a] *Department of Chemistry, School of Science, The University of Tokyo 7-3-1 Hongo, Bunkyo-ku, Tokyo 113-0033, Japan.*

[b] *DYNACOM IRL2015 University of Tokyo - CNRS - Universite de Rennes, Department of Chemistry, 7-3-1 Hongo, Bunkyo-ku, Tokyo 113-0033, Japan.*

*To whom correspondence should be addressed
E-mail: ohkoshi@chem.s.u-tokyo.ac.jp

Contents

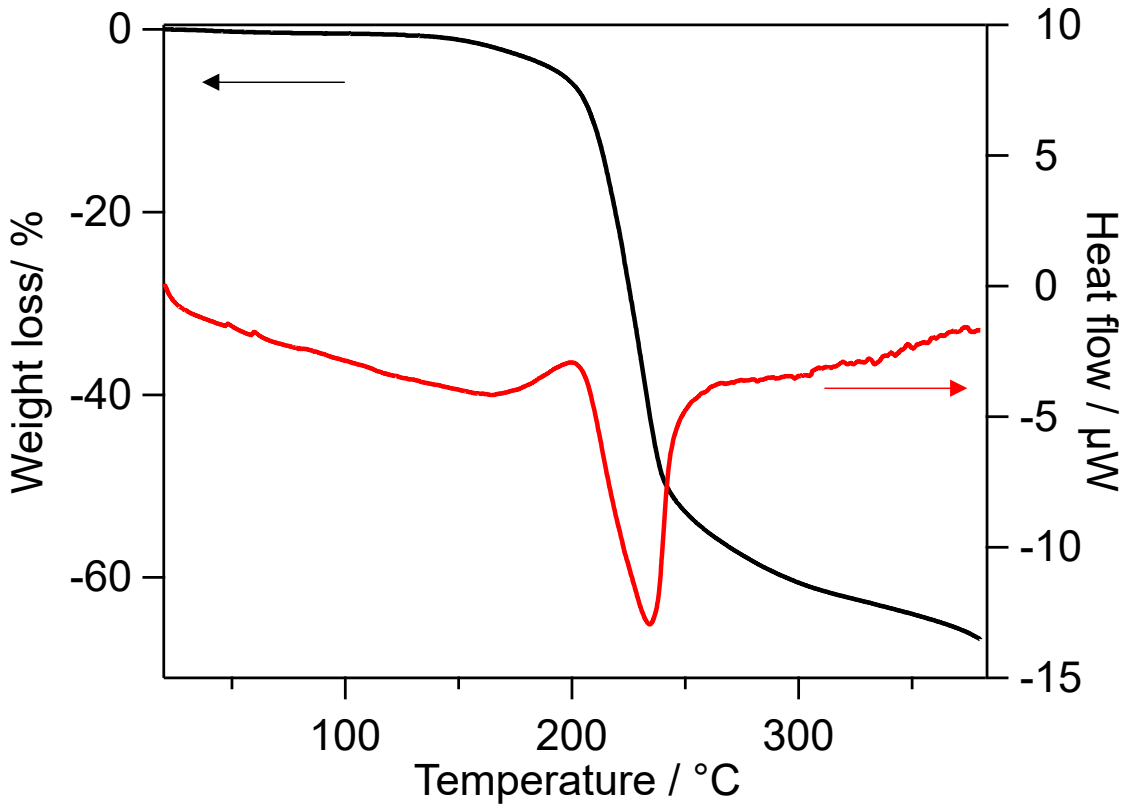

Figure S1. TG-DTA under a scan rate of 5 K min^{-1}. The black and red lines indicate the loss of weight and the heat flow, respectively.

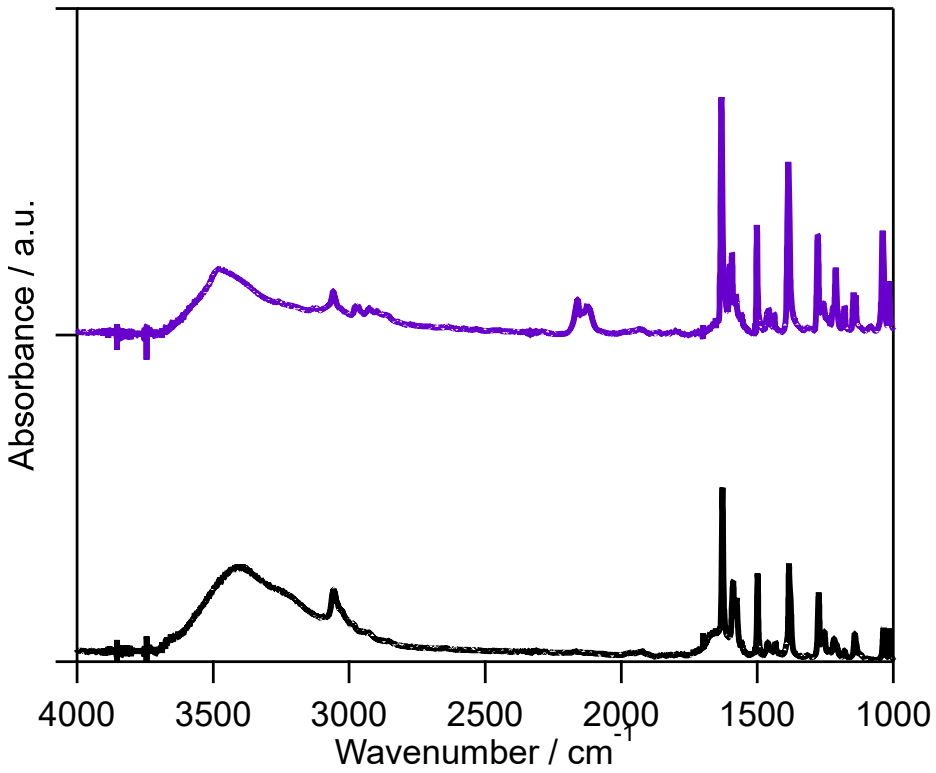

Figure S2. IR spectra of **CoWisoq** at room temperature (top) and isoq (bottom).

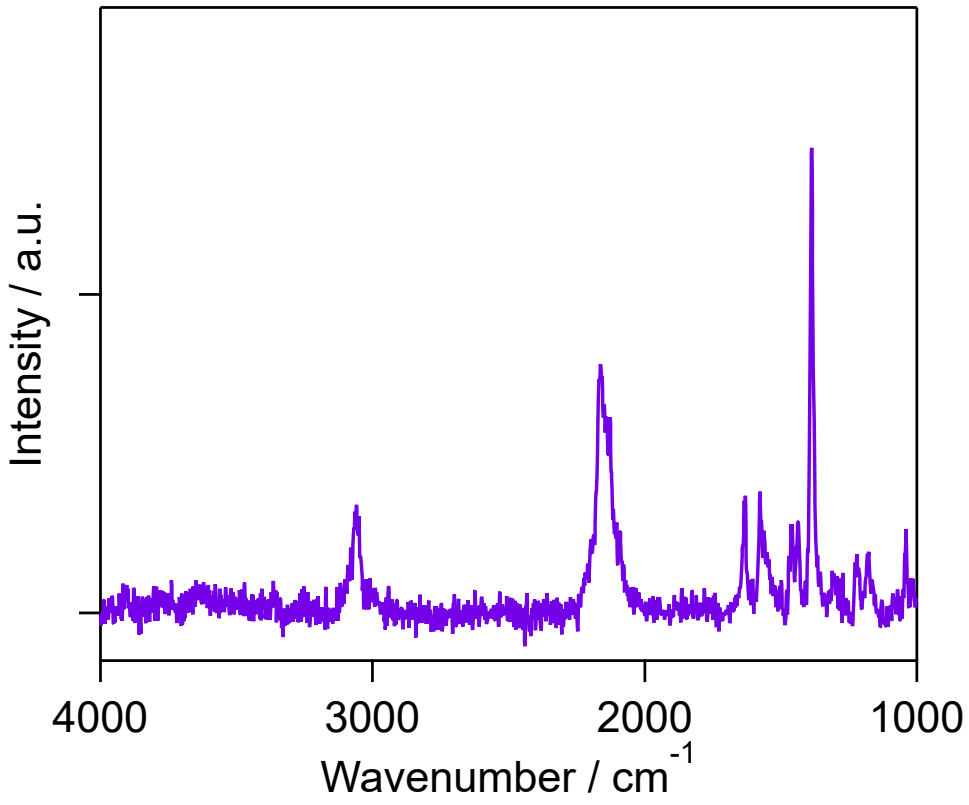

Figure S3. Raman spectrum of **CoWisoq** at room temperature.

Table S1. Crystal data and structure refinement of **CoWisoq** at each temperature.

formula		$Co_3W_2C_{128}H_{96}N_{28}O_2$		
formula weight /g·mol^{-1}		2602.81		
Temperature / K		**90 (2)**	**200 (2)**	**300 (2)**
λ/ Å (Mo Kα)		0.71073		
Crystal system		Monoclinic		
Space group		$P2_1/n$ (#14)		
Unit cell	*a* / Å	14.3610(4)	14.5941(3)	14.6601(4)
	b / Å	26.9695(5)	27.4938(5)	27.5666(5)
	c / Å	15.1714(4)	15.2877(3)	15.3341(4)
	β / Å	113.674(3)	112.698(3)	112.706(3)
V / Å^3		5381.5(3)	5659.1(2)	5716.7(3)
Z		2		
Calcd. density / g cm$_{-3}$		1.606	1.527	1.512
Absorption coeff.		2.653	2.523	2.497
F(000)		2610.0		
Crystal size / mm		0.15 × 0.07 × 0.07		
Crystal type		**Yellow block**	**Purple block**	
θ range / deg		5.048 – 59.208	4.138 – 58.878	3.584 – 58.916
Limiting indices		$-17 \le h \le 19$ $-35 \le k \le 37$ $-20 \le l \le 20$	$-17 \le h \le 20$ $-37 \le k \le 37$ $-20 \le l \le 21$	$-17 \le h \le 20$ $-38 \le k \le 37$ $-20 \le l \le 20$
Collected reflections		77208	85459	89519
Unique reflections		13489	14112	14210
R_{int}		0.0392	0.0353	0.0378
data/restrains/parameters		13489/0/738	14112/0/738	14210/18/738
GOF on F^2		1.170	1.156	1.199
final *R* indices		$R_1 = 0.0335$ $[I > 2\sigma(I)]$ w$R_2 = 0.0667$ (all)	$R_1 = 0.0253$ $[I > 2\sigma(I)]$ w$R_2 = 0.0630$ (all)	$R_1 = 0.0322$ $[I > 2\sigma(I)]$ w$R_2 = 0.0822$ (all)
Largest diff. peak / hole / e·Å^{-3}		2.11 / −1.78	0.87 / −1.21	1.25/−1.66

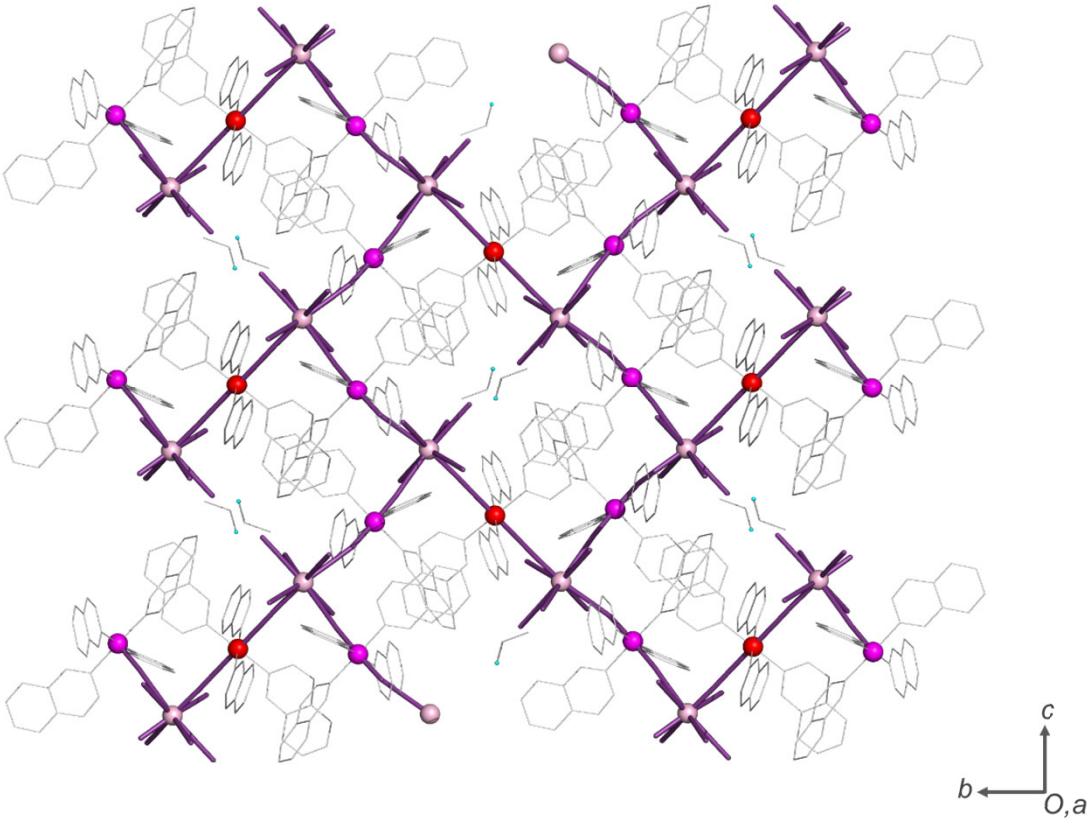

Figure S4. Crystal structure of **CoWisoq** at 300 K viewed from the *a*-axis. The purple, red, pink, and light blue spheres indicate Co1, Co2, W, and O respectively.

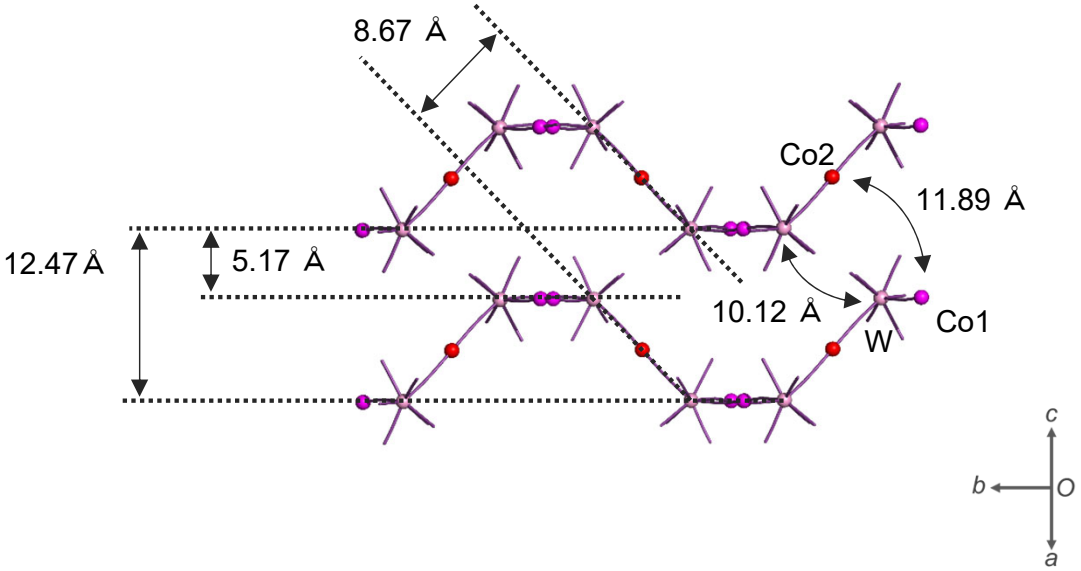

Figure S5. The layered structure of **CoWisoq** viewed from the (101) plane. The distances between the dashed lines represent the distances between the respective planes. The curved arrows indicate [W]···[W] and [Co]···[Co] distances.

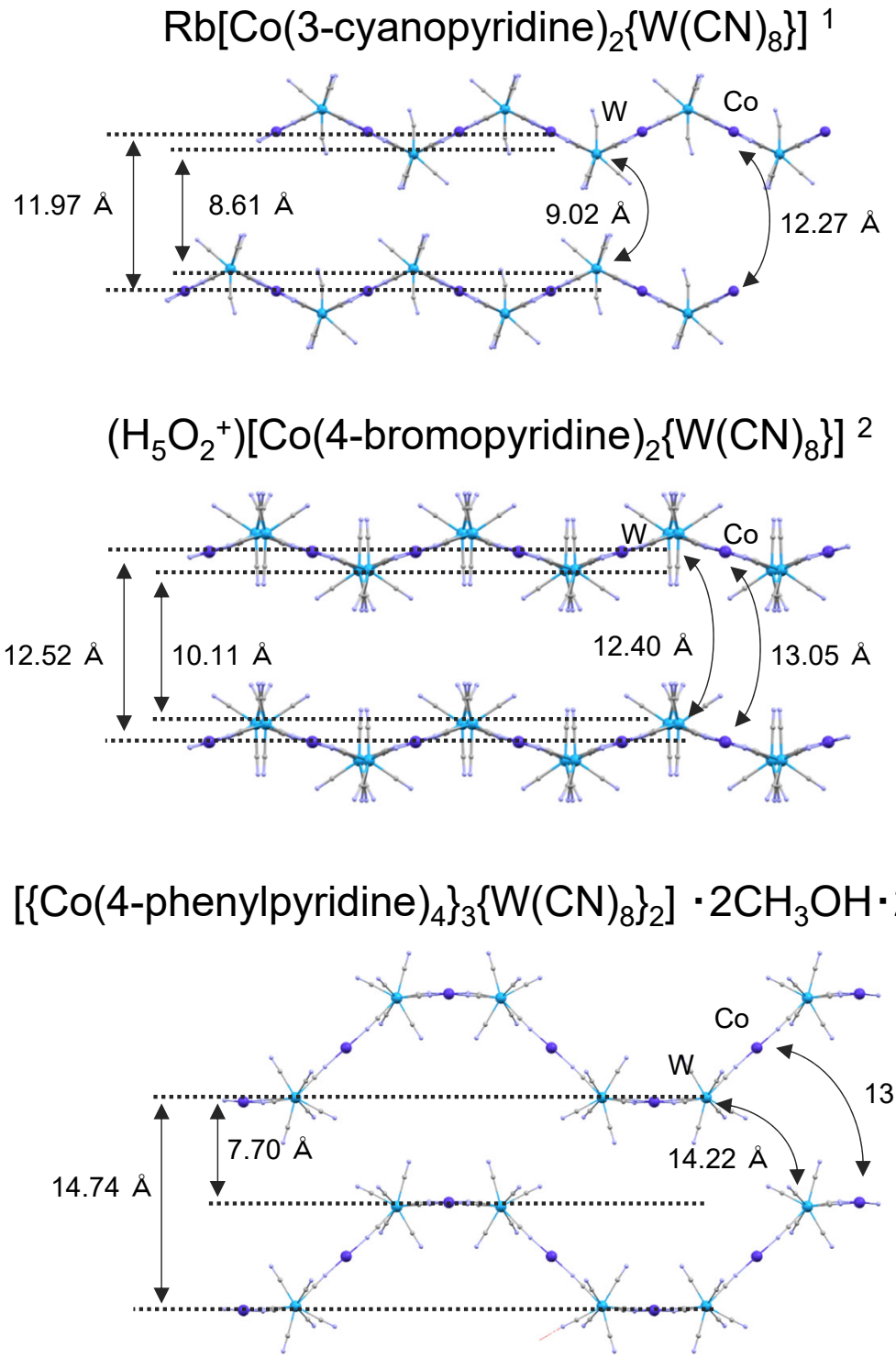

Figure S6. Comparison of the distance between the two-dimensional layers in the previously reported cyanido-bridged Co-W assemblies.

[1]T. Yoshida, K. Nakabayashi, H. Tokoro, M. Yoshikiyo, A. Namai, K. Imoto, K. Chiba and S. Ohkoshi, Extremely low-frequency phonon material and its temperature- and photo-induced switching effects, Chem. Sci., 2020, 11, 8989–8998.

[2]Y. Miyamoto, T. Nasu, N. Ozaki, Y. Umeta, H. Tokoro, K. Nakabayashi and S. Ohkoshi, Photo-induced magnetization and first-principles calculations of a two-dimensional cyanide-bridged Co–W bimetal assembly, Dalton Trans., 2016, 45, 19249–19256.

[3] L. Zhao, R. duan, P.-F. Zhuang, H. Zheng, C.-Q. Jiao, J.-L. Wang, C. He, and T. Liu, 12-Metal 36-membered ring based W^{V}-Co^{II} layers showing spin-glass behavior, Dalton Trans., 2015, 44, 12613–12617.

Table S2. Continuous Shape Measure (CSM) analysis for the $[W(CN)_8]^{n-}$ site in the single crystal of **CoWisoq** at each temperature.

Temperature	CSM parameters*			Geometry
	SAPR-8	BTPR-8	TDD-8	
90 K	2.788	2.192	0.224	TDD-8
200 K	2.910	2.190	0.225	TDD-8
300 K	2.895	2.208	0.223	TDD-8

*CSM parameters

CSM SAPR-8: the parameter related to the Square Antiprism of D_{4d} symmetry

CSM BTPR-8: the parameter related to the Bicapped Trigonal Prism of C_{2v} symmetry

CSM TDD-8: the parameter related to the Dodecahedron of D_{2d} symmetry

CSM = 0 means the ideal geometry, on the contrary, increasing value means the distortion from ideal geometry.

S H A P E v2.1 Continuous Shape Measures calculation
(c) 2013 Electronic Structure Group, Universitat de Barcelona
Contact: llunell@ub.edu

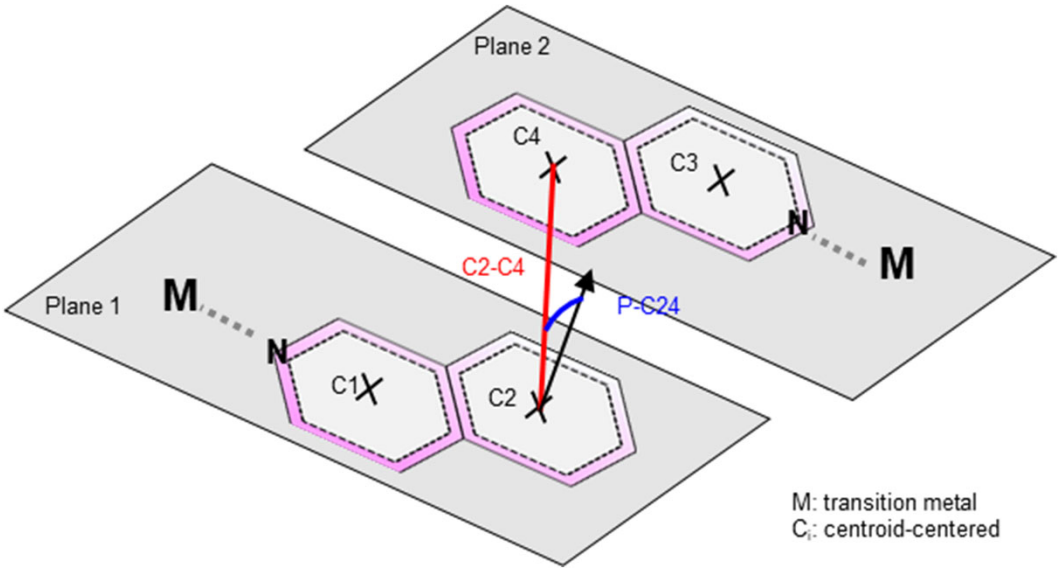

Figure S7. Schematic illustration of the distance and the angle between the isoquinoline ligands with π-π interaction. The arene-arene distance and the displacement angle are defined by the distance between C2 and C4 (red line:C2–C4), and between the normal of the pyridine plane passing through the ring center and the C2–C4 vector (Blue line: P −C24).

Table S3. Distances (Å) of the π-π interaction at each temperature between and in the layer.

temperature	**90 K**	**200 K**	**300 K**
In the layer / Å	3.82	3.92	3.94
Between the layer / Å	3.54	3.64	3.67

Table S4. Displacement angles (º) of the π-π interaction at each temperature between and in the layer.

temperature	**90 K**	**200 K**	**300 K**
In the layer / º	20.89	18.34	17.47
Between the layer / º	19.63	16.17	15.94

Table S5. Bond lengths (Å) between Co and N atoms in the crystal structure **CoWisoq** at each temperature. $Co–N_A$ and $Co–N_E$ indicate the average distance between Co and nitrogen in the axial and the equatorial positions, which are from cyanides and isoq, respectively.

temperature	**90 K**	**200 K**	**300 K**
$[Co1(isoq)_4(NC)_2]$			
$Co1–N_A$ / Å	1.903 (7)	2.100 (4)	2.107 (6)
$Co1–N_E$ / Å	1.985 (5)	2.168 (14)	2.174 (11)
$[Co2(isoq)_4(NC)_2]$			
$Co2–N_A$ / Å	2.093 (2)	2.116 (2)	2.123 (2)
$Co2–N_E$ / Å	2.202 (9)	2.197 (10)	2.199 (6)

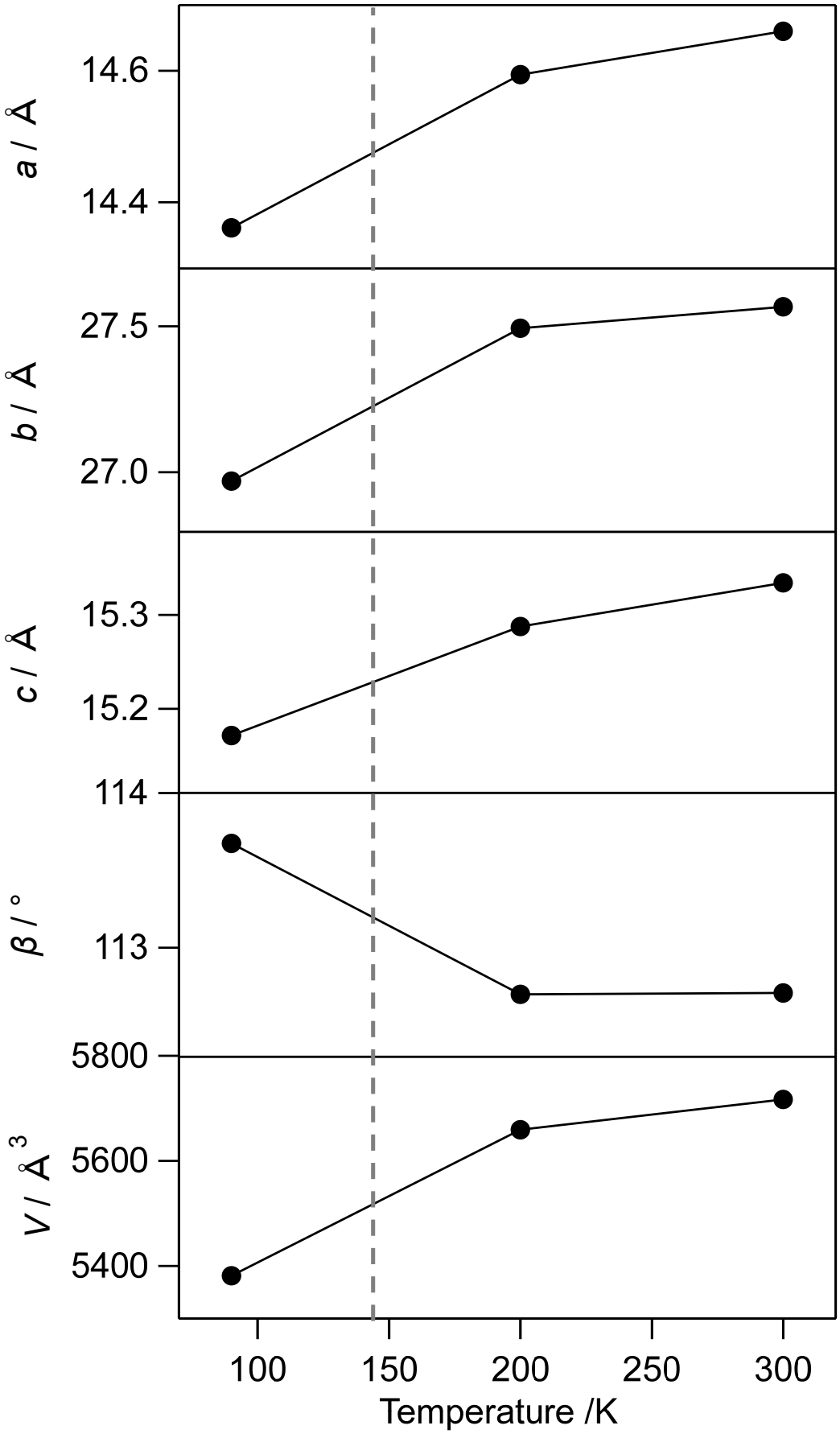

Figure S8. Temperature dependences of the lattice constants of **CoWisoq**. Gray dashed line indicates the transition temperature.

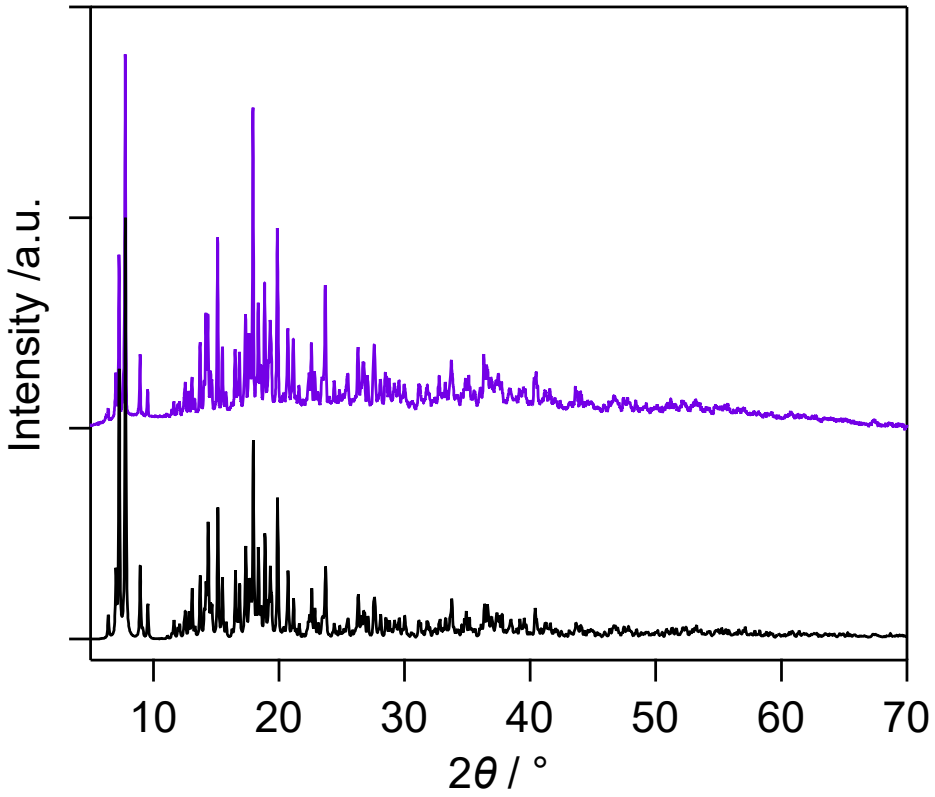

Figure S9. PXRD pattern the sample with ground crystals of **CoWisoq** at room temperature. Purple and black lines represent the experimental data and calculated pattern from the crystal structure of the single crystal at 300 K.

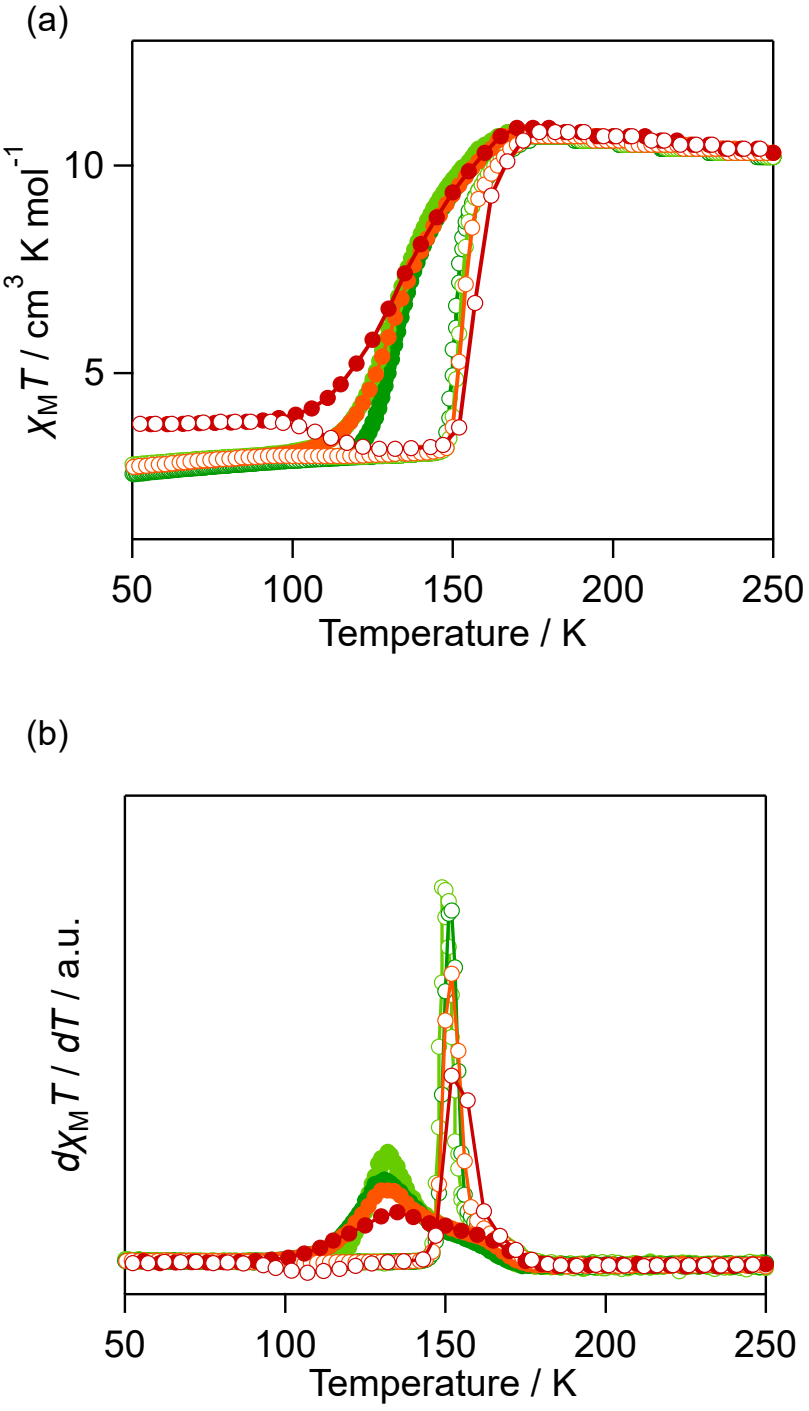

Figure S10. Temperature dependences of the $\chi_M T$ products of **CoWisoq** under 5000 Oe on cooling (filled circle) heating (open circle) for the range of 50 to 250 K. (a) $\chi_M T$ –T plots. (b) the first derivative of $\chi_M T$ vs T plots. Red, orange, light green, and green circles indicate sweep rate at 5.0, 2.0, 1.0, and 0.5 K min^{-1}, respectively

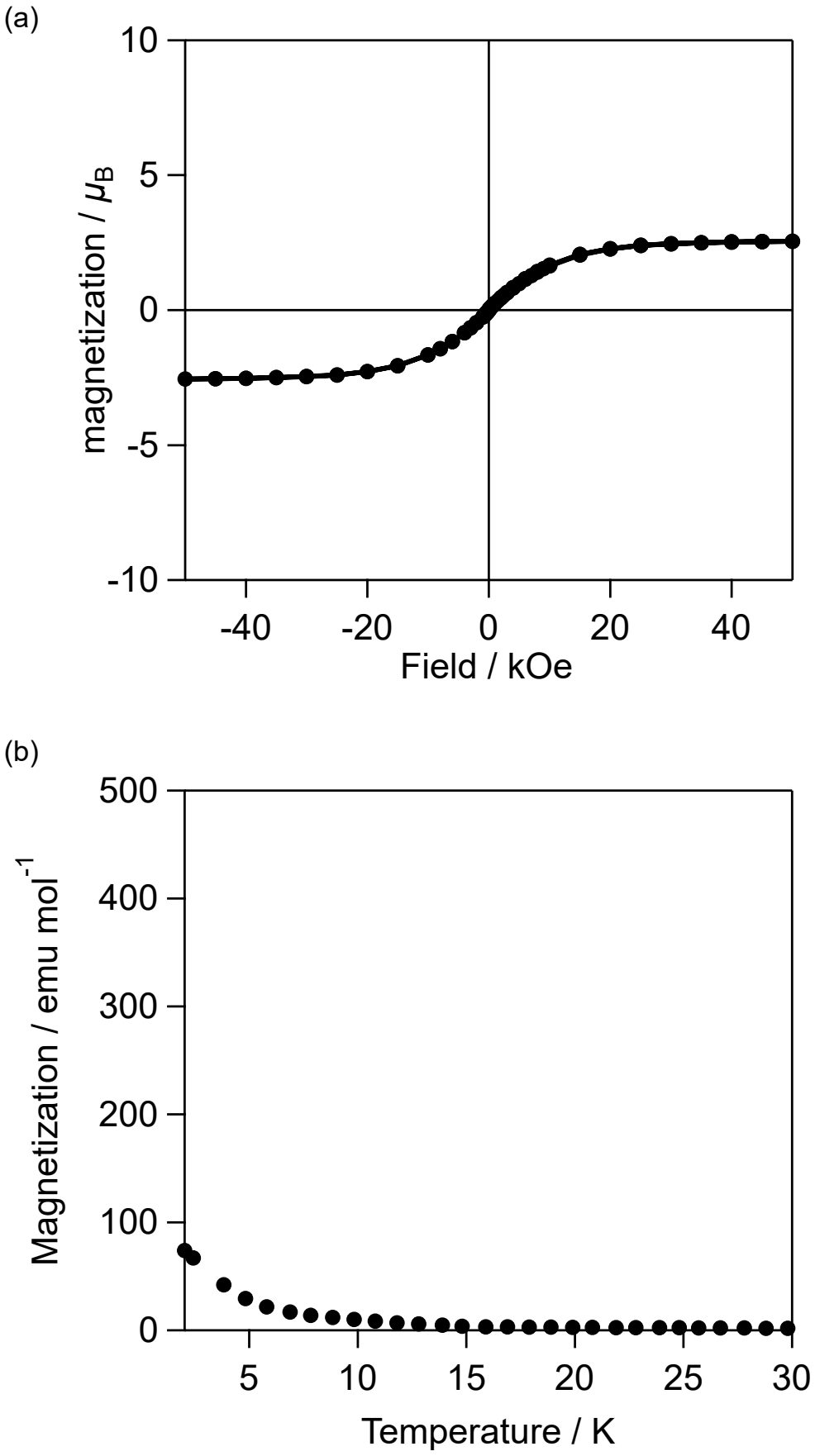

Figure S11. Magnetic properties of the LT phase of **CoWisoq**. (a) *M–H* curve at 2 K. (b) FCM curve under 20 Oe.

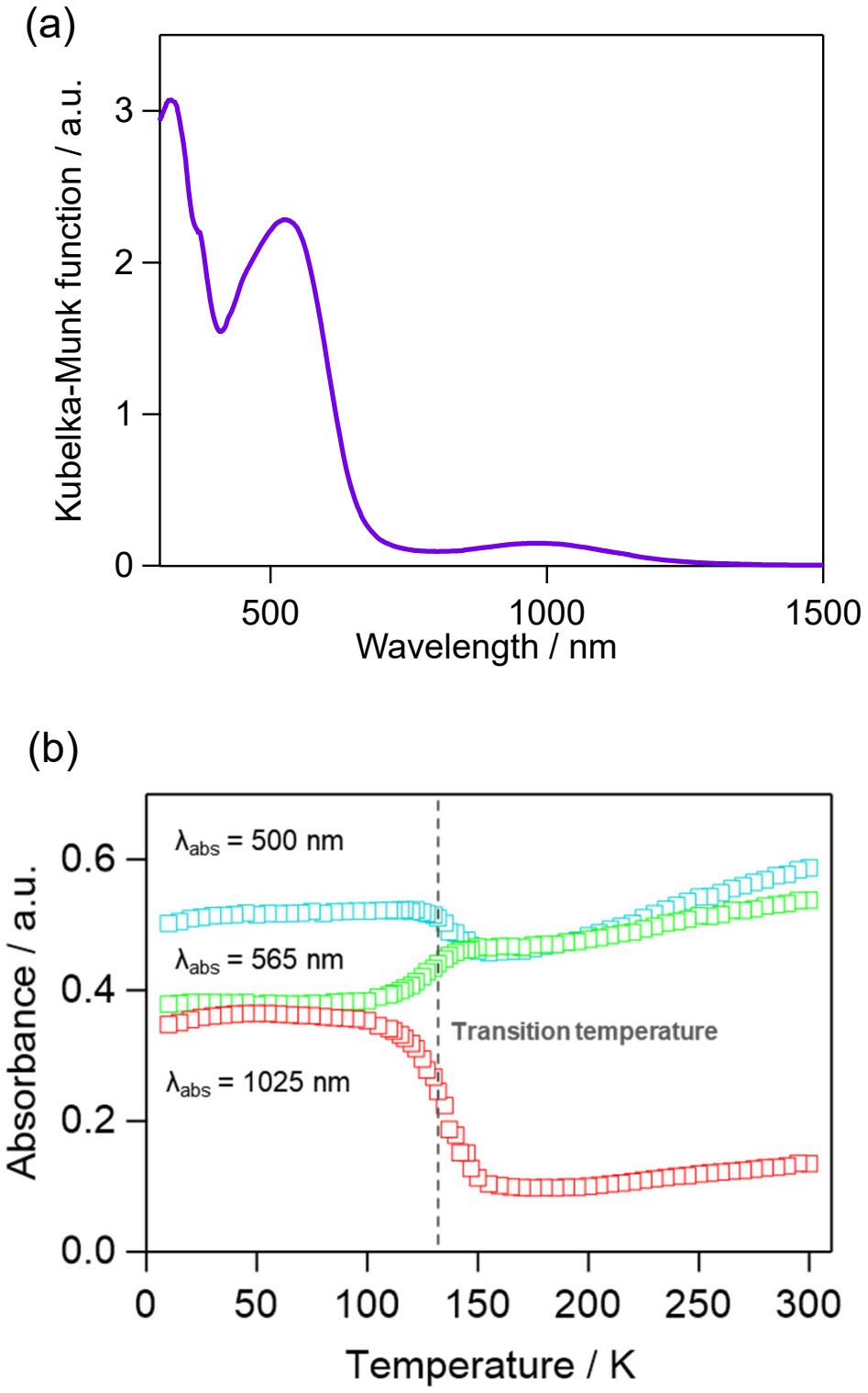

Figure S12. (a) UV-vis-NIR spectrum of **CoWisoq** in the range of 350–1500 nm at room temperature. (b) Temperature dependencs of the absorbance at 500 nm (light blue), 565 nm (light green), and 1025 nm (red).

Table S6. MMCT bands from W^{IV} to Co^{III} in the cyanido-bridged Co–W photomagnets.

Compounds	λ /nm	[ref.]
$[\{Co(Isoquinoline)_4\}_3\{W(CN)_8\}_2]\cdot 2EtOH$	1025	Present work
$Co_3[W(CN)_8]_2(Pyrimidine)_4\cdot 6H_2O$	772	37
$Co_3[W(CN)_8]_2(Pyrimidine)_2(4\text{-}Methlpyridine)_2\cdot 6H_2O$	742	38
$Rb[Co(3\text{-}Cyanopyridine)_2\{W(CN)_8\}]$	780	30
$(H_5O_2^+)[Co(4\text{-}Bromopyridine)_2[\{W(CN)_8\}]$	700	39
$Cs^+_{0.1}(H_5O_2^+)_{0.9}[Co(4\text{-}Bromopyridine)_{2.3}[\{W(CN)_8\}]$	760	40

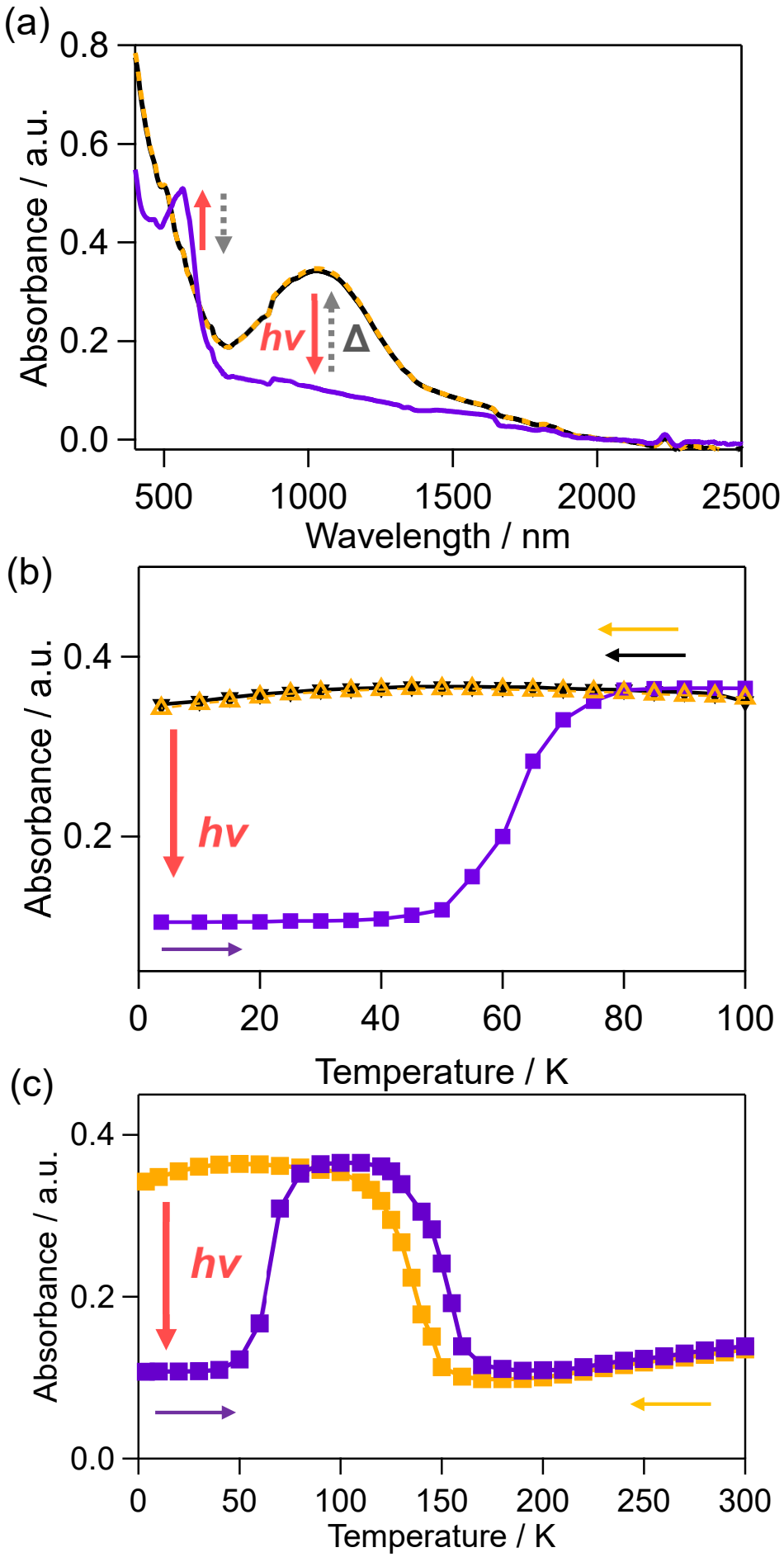

Figure S13. (a) UV-vis-NIR spectra at 3.8 K before (black line), after (purple line) photo irradiation (980 nm, 46mW cm^{-2}, 5 min), and after thermal annealing at 100 K (yellow dash line). (b) Temperature dependence of the absorbance at 1025 nm upon initial cooling (black), heating after irradiation (purple), and second cooling (yellow). (c) Temperature dependence of the absorption at 1025 nm upon cooling (yellow) and heating after irradiation (purple).

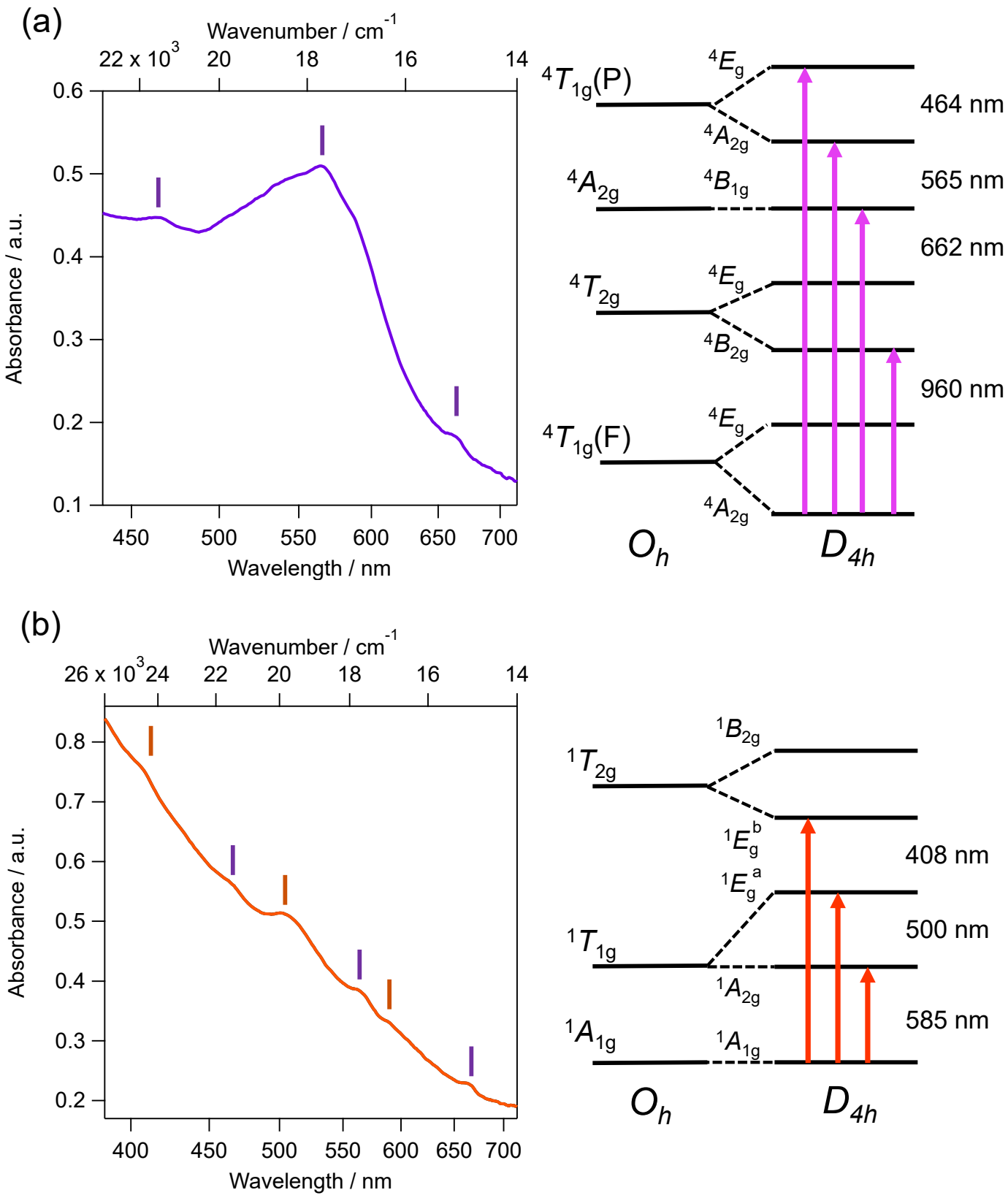

Figure S14. Attribution of the d-d transitions of Co of **CoWisoq** in the UV-vis-NIR spectrum at 3.8 K and the schematic energy diagrams (a) after photo irradiation for Co^{II}, and (b) before photo irradiation for Co^{III}. Purple and orange bars indicate the peak originated from the d-d transitions of Co^{II} and Co^{III}.

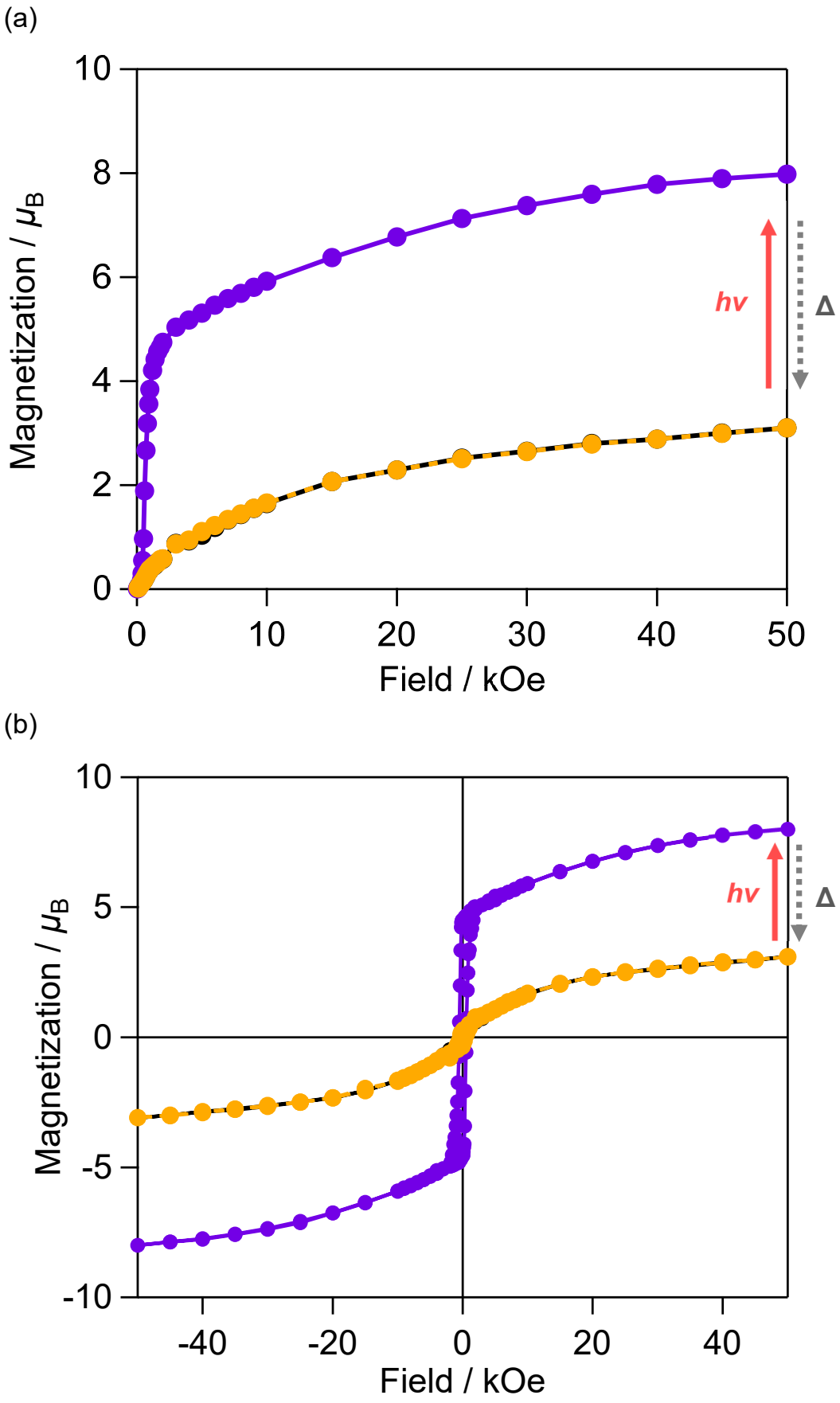

Figure S15. Photo-induced magnetization of **CoWisoq**. Initial *M–H* curve at 2 K (a) and Magnetic hysteresis loop at 2 K (b) before (black) and after (purple) irradiation, and after thermal annealing at 100 K (yellow) in the range of 50 to −50 kOe.

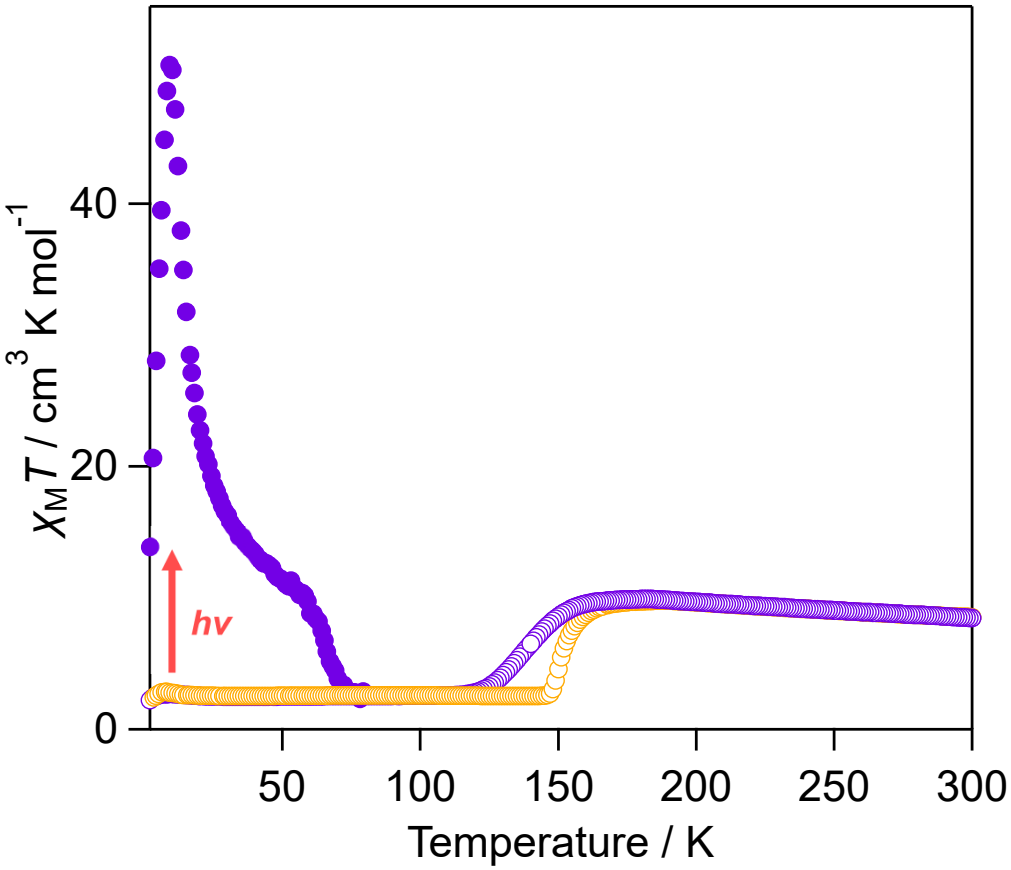

Figure S16. Temperature dependence of the $\chi_M T$ product of **CoWisoq** upon cooling (purple-open circle) heating (yellow circle) and after photoirradiation heating (purple-filled circle).

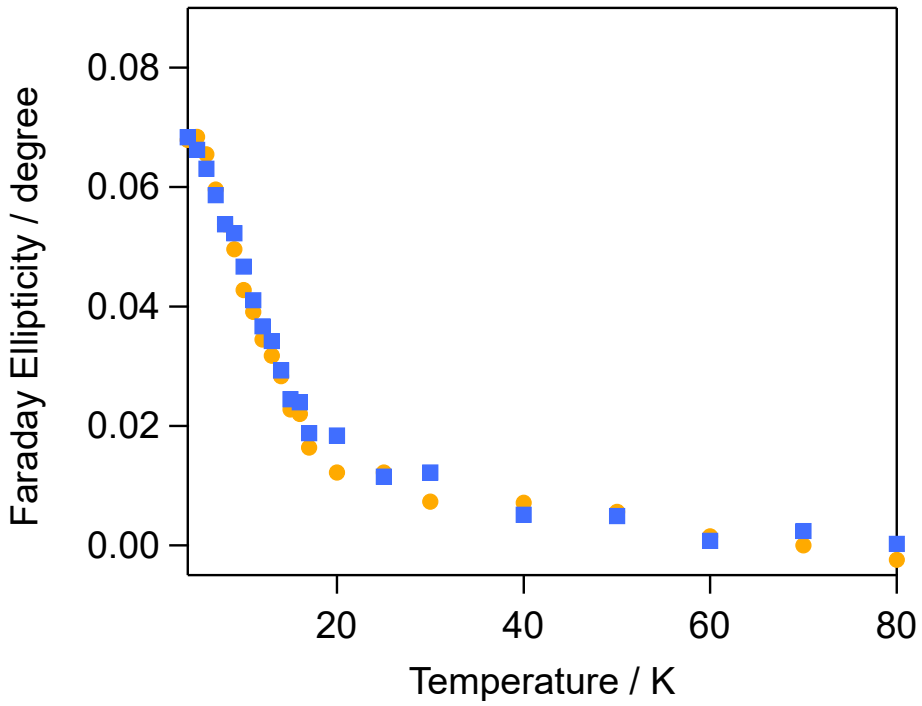

Figure S17. Temperature dependence in the variable-temperature Faraday ellipticity of the PI phase in **CoWisoq** by applying a magnetic field of 10 kOe at 390 (blue square) and 550 nm (orange circle).

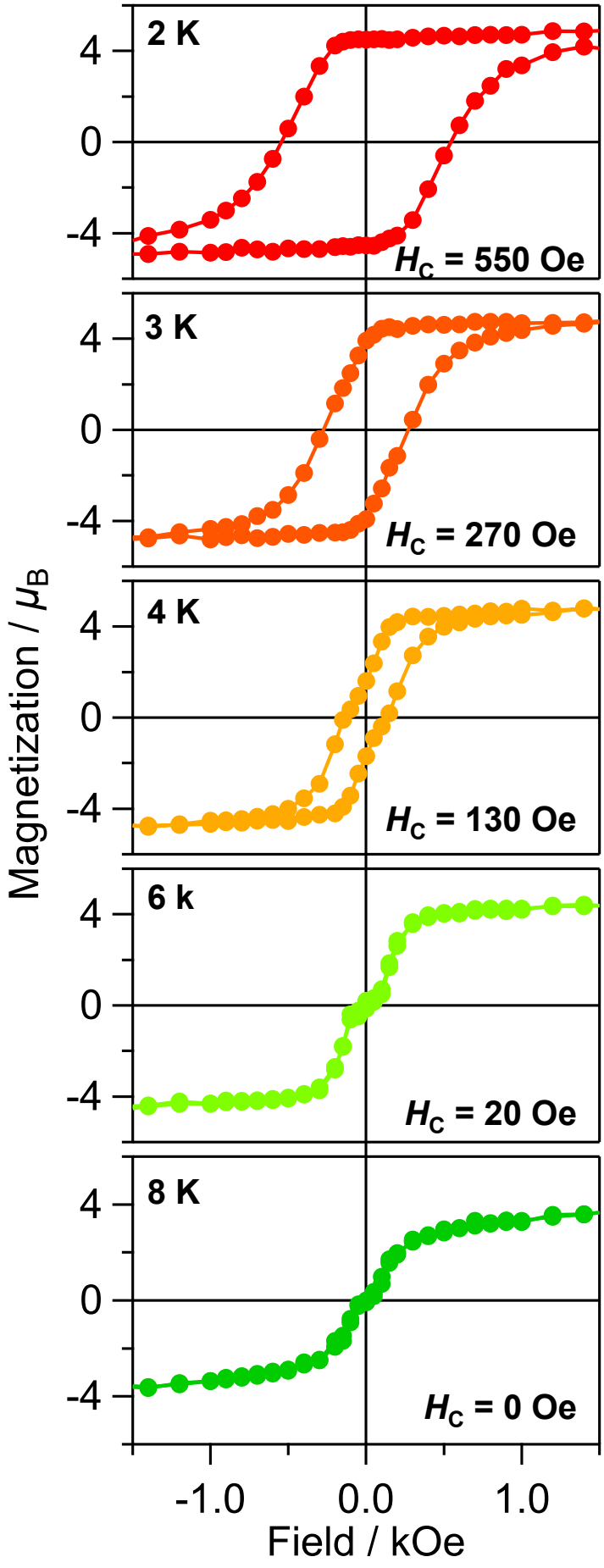

Figure S18. (a) Magnetic hysteresis loops of the photo-induced phase in the range of −1.5 to 1.5 kOe at respective temperatures. Red, orange, light orange, light green, and green indicate at 2, 3, 4, 6, and 8 K, respectively.

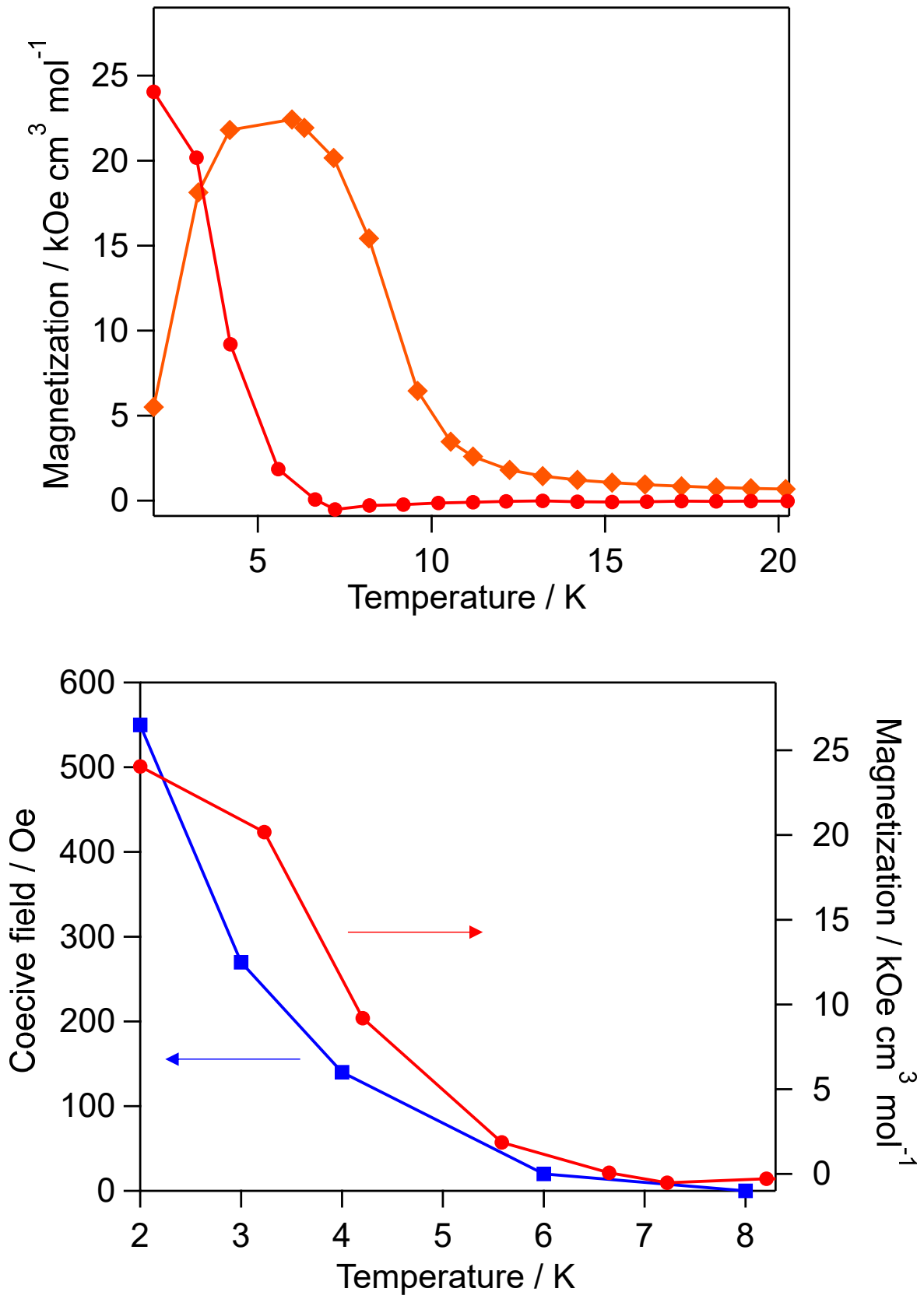

Figure S19. ZFCM (orange circle) curve of the PI phase of **CoWisoq** under an external magnetic field of 500 Oe, and remnant magnetization (red circle) curve under 0 Oe in the PI phase of **CoWisoq**. (b) Temperature dependence of the remnant magnetization and the coercive field (H_C).

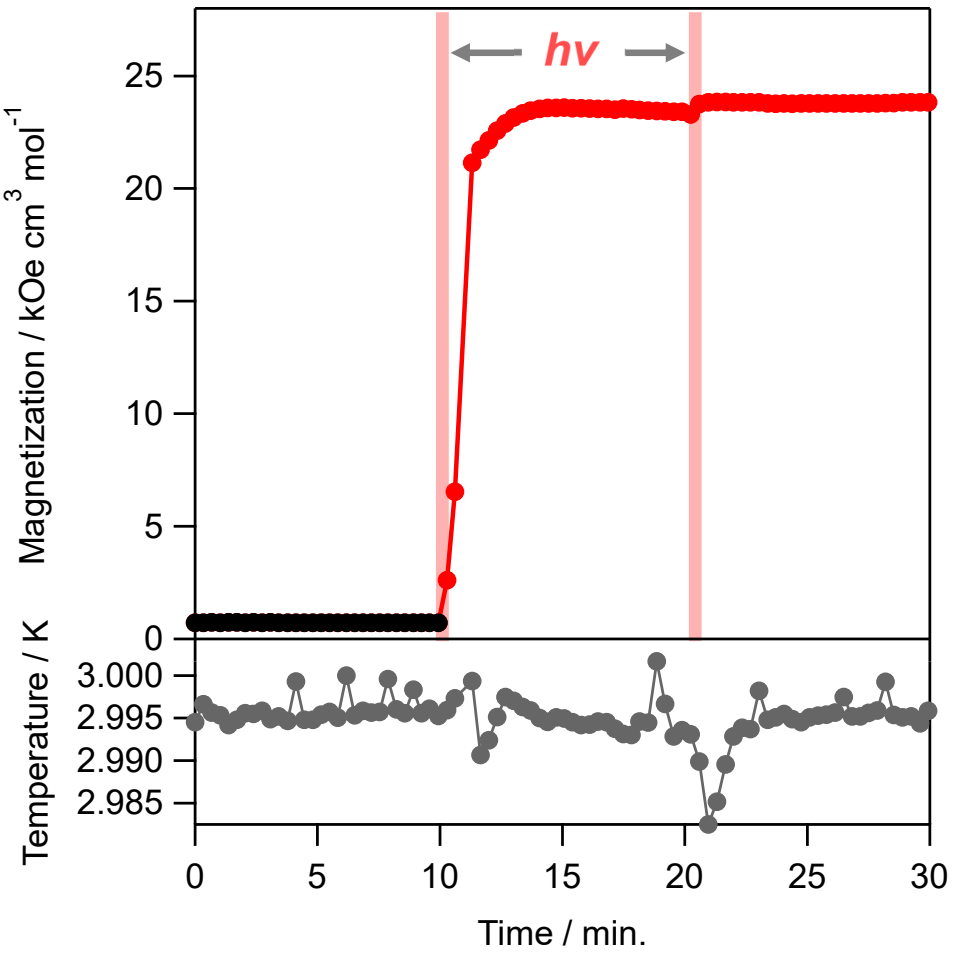

Figure S20. Photo–induced magnetization of **CoWisoq** by 1064 nm (82 mW cm^{-2}, 10 min) vs time plot under 500 Oe at 3 K. Black, red, and gray cercle present the magnetization before and after photo irradiation, and temperature inside the sample chamber measured by the MPMS.

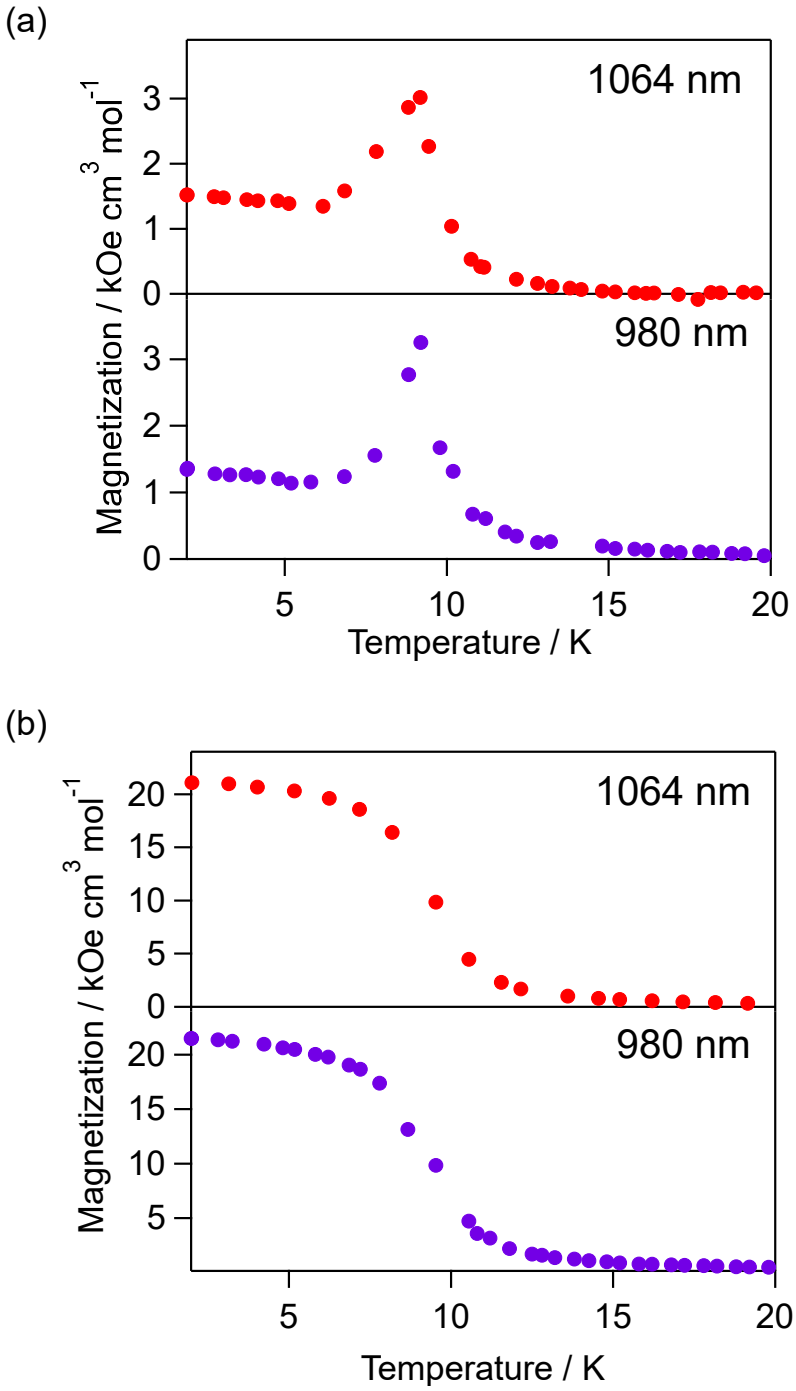

Figure S21. Photo–induced magnetization of **CoWisoq**. Magnetization vs. temperature curves under (a) 100 Oe, and (b) 500 Oe. Red and purple circles indicate the photo irradiation of 1064 nm (82 mW cm^{-2}, 10 min) and 980 nm (26 mWcm^{-2}, 30 min), respectively.